Supplementary Information

A mini-review on performance metrics for electrochemically mediated ammonia recovery from wastewater

Weikun Chen[1,2] and Taeyoung Kim[3,4*]

[1]School of Life and Environmental Science, Wenzhou University, Wenzhou, Zhejiang, 325035, China
[2]Zhejiang Provincial Engineering Laboratory of Ecological Treatment Technology for Urban Water Pollution, Wenzhou, Zhejiang, 325035, China
[3]Institute for a Sustainable Environment, Clarkson University, Potsdam, NY, 13699, United States
[4]Department of Chemical and Biomolecular Engineering, Clarkson University, Potsdam, NY, 13699, United States
[*]Corresponding Author: tkim@clarkson.edu

Table S1. Detailed parameters for calculation of productivity.

Sources	Initial ammonia concentration (mM)	Projected area (cm^2)	Flow rate (mL min^{-1})[a]	Nitrogen flux (g N m^{-2} d^{-1})	Current density (A m^{-2})	Ammonia removal	Membranes used[b]	Productivity (mmol N g^{-1} membrane h^{-1})*	Energy consumption (kWh kg^{-1} N)	References
Electrolysis										
Anaerobic digestate	151	64	0.3	51	10	38%	1 CEM	1.2	13.1	1
				90	20	58%		2.0	16.7	
				94	30	63%		2.1	26.0	
Urine	364	64	0.3	235	40	76%	1 CEM	5.3	14.7	2
	343			275		75%		6.2	12.7	
Source-separated urine	392	100	0.6	N.A.[c]	20	87%	1 CEM	9.1	2.9[e]	3
						67%[d]		7.0	3.6	
Urine	243	100	0.2	78	10	82%	1 CEM	1.8	8.5	4
			0.4	151	20	73%		3.4	7.3	
			1.0	342	50	73%		7.7	15.6	
Urine	236	100	0.2	82	20	89%	1 CEM	1.8	4.0	5
			1.1	335	50	63%		7.6	3.9	
			0.2	89	50	92%		2.0	13.2	
Urine	535	64	1.7	1710	100	60%	1 CEM	38.6	8.5	6
Urine	330	100	0.9	N.A.[c]	20	49%	1 CEM	6.4	4.6	7
						45%		5.8	5.9	
Anaerobic digestate	263	40	1.1	N.A.[c]	200	86%[f]	1 CEM	28.4	11.6	8

Sources	Initial ammonia concentration (mM)	Projected area (cm^2)	Flow rate (mL min^{-1})[a]	Nitrogen flux (g N m^{-2} d^{-1})	Current density (A m^{-2})	Ammonia removal	Membranes used[b]	Productivity (mmol N g^{-1} membrane h^{-1})*	Energy consumption (kWh kg^{-1} N)	References
Anaerobic digestate	57	10	0.1	N.A.[c]	13	99%[g]	1 CEM 1 AEM	1.3	8.2	9
			0.2		25	99%[g]		2.7	12.2[h]	
			0.4		50	98%[g]		5.3	17.0[h]	
			0.6		75	96%[g]		7.8	19.7[h]	
			0.8		100	94%[g]		9.2	29.5	
Urine	360	64	0.5	N.A.[c]	100	83%	1 CEM	10.7	17.0	10
Synthetic livestock wastewater	200	40	1.7	N.A.[c]	63	23%	1 CEM	8.8	8.7	11
					125	38%		14.3	13.1[i]	
					250	48%		18.1	23.6[i]	
Bipolar membrane electrodialysis										
Synthetic sludge reject water	84	64	1.1	N.A.[c]	N.A.[c]	85%	1 CEM 1 AEM 1 BPM	1.4	5.3	12
Synthetic dewatering centrate	111	100	1.2	202	25	81%	1 CEM 1 BPM	1.5	3.4	13
			2.3	364	50	74%		2.7	4.7	
			4.7	819	100	78%		6.2	5.1	
Dewatering centrate	85	37	2.4	N.A.[c]	26 V[j]	60%[k]	1 CEM 1 BPM	5.0	16.1[l]	14
			2.4		35 V[j]	95%		7.9	13.0[k]	
			4.8		35V[j]	87%		14.5	7.7	
			4.8		26 V[j]	43%[k]		7.1	11.5[l]	

Sources	Initial ammonia concentration (mM)	Projected area (cm^2)	Flow rate (mL min^{-1})[a]	Nitrogen flux (g N m^{-2} d^{-1})	Current density (A m^{-2})	Ammonia removal	Membranes used[b]	Productivity (mmol N g^{-1} membrane h^{-1})*	Energy consumption (kWh kg^{-1} N)	References
Dewatering centrate	85	37	5.7	N.A.[c]	30 V[j]	50%	1 CEM 1 BPM	10.0	14.4[m]	15
			4.5			60%		9.4	15.0	
			3.0			70%		7.3	18.7[m]	
			3.2		20 V[j]	50%		5.7	9.6[m]	
			2.4			60%		5.0	10.2[m]	
			1.2			70%		2.9	17.8[m]	
Synthetic urine	269	50	1.2	739	200	68%	1 CEM 1 AEM 1 BPM	4.2	7.2[n]	16
Anaerobic digestate	35	484	24.2	179	50	53%	1 CEM 1 BPM	1.3	11.8	17
			31.1	144	50	34%[o]		1.1	17.7	
			36.2	193	75	41%[o]		1.5	35.8	
Synthetic dewatering centrate	50	29	1.7	431	84	75%	1 CEM 1 AEM 1 BPM	2.4	8.0[n]	18
			1.0	264	51	76%		1.5	5.9[n]	
Flow-electrode capacitive deionization										
Synthetic domestic wastewater	2.9	35	2.6	36	12	79%[p]	1 CEM 1 AEM	0.4	6.0[q]	19
			1.7	27	12	90%[p]		0.3	13.1[q]	
			1.3	22	12	96%[p]		0.2	25.1[q]	
Domestic wastewater	3.0	58	1.7	13	6.8	75%[r]	1 CEM 1 AEM	0.1	18.9[t]	20
Synthetic urine	268		0.4	265	27	82%[s]		3.0	7.8[t]	

Sources	Initial ammonia concentration (mM)	Projected area (cm^2)	Flow rate (mL min^{-1})[a]	Nitrogen flux (g N m^{-2} d^{-1})	Current density (A m^{-2})	Ammonia removal	Membranes used[b]	Productivity (mmol N g^{-1} membrane h^{-1})*	Energy consumption (kWh kg^{-1} N)	References
Synthetic domestic wastewater	1.4	35	1.8	N.A.[c]	1.2 V[j]	87%	1 CEM 1 AEM	0.1	4.7[u]	21
Synthetic domestic wastewater	3.1	35	1.7	N.A.[c]	6.0	75%[v]	1 CEM 1 AEM	0.3	35.4	22
Synthetic gray water	18	24	1.0	N.A.[c]	9.8	41%	1 CEM 1 AEM	0.7	4.5	23
						60%		1.1	2.0	
Proton-coupled electron transfer										
Synthetic domestic wastewater	5.0	7	0.5	30	4.8	44%[w]	2 CEMs	0.3	1.2	24
				34	9.6	50%[w]		0.4	3.2	
				39	19	57%[w]		0.4	12.6	
Prussian blue analogues (electrode)										
Domestic wastewater	3.4	7	0.3	N.A.[c]	0.2 V[j]	85%	1 AEM	0.6	1.5	25
Synthetic domestic wastewater	5.0	7	0.3	N.A.[c]	0.3 V[j]	100%	1 AEM	1.0	2.4	26
Synthetic domestic wastewater	5.0	7	0.3	N.A.[c]	0.3 V[j]	100%	1 AEM	1.0	1.0	27
	10					70%		1.4	0.6	
	17					47%		1.6	0.4	

Sources	Initial ammonia concentration (mM)	Projected area (cm^2)	Flow rate (mL min^{-1})[a]	Nitrogen flux (g N m^{-2} d^{-1})	Current density (A m^{-2})	Ammonia removal	Membranes used[b]	Productivity (mmol N g^{-1} membrane h^{-1})*	Energy consumption (kWh kg^{-1} N)	References
Synthetic domestic wastewater	5.0	9	3	N.A.[c]	0.5 V[j]	80%	1 AEM	6.1	1.1	28
Synthetic domestic wastewater	10	64	9	N.A.[c]	0.1 V[j]	21%[x]	1 AEM	1.3	0.2[y]	29
					0.4 V[j]	63%[x]		4.0	1.1[y]	
					0.8 V[j]	78%[x]		5.0	2.1[y]	
					1.2 V[j]	57%[x]		3.6	5.3[y]	
Prussian blue analogues (membrane)										
Synthetic domestic wastewater	5.0	7	0.3	13[aa]	3.4	42%	1 CEM	0.3	11.8	30
Domestic wastewater	4.4[z]	7	0.3	21[aa]	3.4	64%		0.5	9.9	

*Productivity was calculated using Eq. 1 in the main text, wherein the concentration of separated ammonia was calculated from the initial ammonia concentration and ammonia removal.

[a]For batch mode experiments, the flow rate was calculated based on the volume of treated wastewater, the running time, and the number of repeating units.

[b]For multiple cell-pair configurations, the repeating unit was considered.

[c]Not available.

[d]Estimated from Figure 2.

[e]Estimated from SI Table S7.

[f]Estimated from Figure 4a.

[g]Estimated from Figure 2a.

[h]Estimated from Figure 3a.

[i]Estimated from Figure 2d.

[j]Applied voltage.
[k]Estimated from Figure 3.
[l]Estimated from Figure 5.
[m]Estimated from Figure 7.
[n]Excluding energy for electrodes.
[o]Estimated from Figure 2a.
[p]Estimated from Figure 3b.
[q]Estimated from SI Table S1.
[r]Estimated from SI Figure S9a.
[s]Estimated from SI Figure S10.
[t]Estimated from Figure 5b.
[u]Estimated from Figure 5d.
[v]Estimated from SI Figure S1b.
[w]Estimated from Figure 3d.
[x]Estimated from SI Figure S5a.
[y]Estimated from Figure 3c.
[z]Estimated from Figure 3.
[aa]Estimated from Figure 2a.

Table S2. Productivity and capital-cost-based productivity for Fe-based Haber-Bosch processes from literature.

Catalysts	Productivity (mmol N g^{-1} catalyst h^{-1})	Productivity (mmol N $\$^{-1}$ catalyst h^{-1})[a]	Capital-cost-based productivity (mmol N $\$^{-1}$ h^{-1})[b]	References
7% Fe/CeO_2	0.2	7.8	0.04	31
20% $Fe–BaH_2$	1.7	85.2	0.4	32
2.8% Fe/γ-Al_2O_3	1.2×10^{-4}	6×10^{-3}	3×10^{-5}	33
Fe (95%) Co (5%)	0.8	41	0.2	34
1.2% $Fe/BaCeO_{3-x}H_yN_z$	6.8	340	1.7	35
$Fe_{91}Zr_9$	0.07	3.6	0.02	36
Fe–5LiH	4.8	242	1.2	37
Fe/LiH	11.4	571.4	2.9	38
10% Fe/C	14.4	720	3.6	39
80% $Fe/Ce_{0.8}Sm_{0.2}O_{2-\delta}$	8.7	435	2.2	40
FePc	14	700	3.5	41
Fe-Metal organic framework	30.4	1520	7.6	42
$Fe_{1-x}O$	11.9	595	3.0	43
1% $Fe/BaTiO_{3-x}H_x$	14	700	3.5	44
$FeOOH/Al_2O_3$	32.9	1642.5	8.2	45
FeO Fe^{2+}/Fe^{3+} = 4.62	96.5	4825	24.1	46
Fe-cat. (KMI)	37.8	1890	9.5	47
A301 catalyst (FeO)	22.3	1115	5.6	48
Fe-based K/Fe/MWNT	0.1	6.5	0.03	49
KMI (Fe catalyst)	33.5	1674.1	8.4	50
Average	17.1	855.7	4.3	

[a]The productivity (mmol N $\$^{-1}$ catalyst h^{-1}) was converted from the mass-based productivity (mmol N g^{-1} catalyst h^{-1}) the price of KM1R (0.02 USD/g).[51]

[b]The capital-cost-based productivity (mmol N $\$^{-1}$ h^{-1}) was converted from the productivity (mmol N $\$^{-1}$ h^{-1}) based on the ratio of catalyst to capital cost in iron-based Haber-Bosch process (0.5%).[52]

Table S3. Productivity and capital-cost-based productivity for IEM-based electrochemical processes.

References	Productivity (mmol N m^{-2} h^{-1})	Membranes used[a]	Productivity (mmol N $\$^{-1}$ membrane h^{-1})[b]	Capital-cost-based productivity (mmol N $\$^{-1}$ h^{-1})[c]
Electrolysis				
1	152.6	1 CEM	2.5	0.5
	266.8		4.4	0.9
	281.0		4.7	1.0
2	699.4	1 CEM	11.7	2.4
	818.5		13.6	2.9
3	1198.4	1 CEM	20.0	4.2
	921.9		15.4	3.2
4	233.0	1 CEM	3.9	0.8
	449.4		7.5	1.6
	1018.2		17.0	3.6
5	244.0	1 CEM	4.1	0.9
	997.0		16.6	3.5
	264.9		4.4	0.9
6	5089.3	1 CEM	84.8	17.8
7	849.3	1 CEM	14.2	3.0
	767.6		12.8	2.7
8	3748.3	1 CEM	62.5	13.1
9	352.1	1 CEM 1 AEM	2.9	0.6
	704.3		5.9	1.2
	1397.1		11.6	2.4
	2059.3		17.2	3.6
	2441.6		20.3	4.3
10	1407.4	1 CEM	23.5	4.9

References	Productivity (mmol N m^{-2} h^{-1})	Membranes used[a]	Productivity (mmol N $\$^{-1}$ membrane h^{-1})[b]	Capital-cost-based productivity (mmol N $\$^{-1}$ h^{-1})[c]
11	1155	1 CEM	19.3	4.0
	1882.5		31.4	6.6
	2385		39.8	8.3
Average	1222.5		18.1	3.8
Bipolar membrane electrodialysis				
12	748.0	1 CEM, 1 AEM, 1 BPM	3.1	0.7
13	601.5	1 CEM 1 BPM	3.3	0.7
	1081.8		6.0	1.3
	2437.8		13.5	2.8
14	1983.3	1 CEM 1 BPM	11.0	2.3
	3140.2		17.4	3.7
	5751.5		32.0	6.7
	2822.9		15.7	3.3
15	3966.6	1 CEM 1 BPM	22.0	4.6
	3718.7		20.7	4.3
	2892.3		16.1	3.4
	2253.7		12.5	2.6
	1983.3		11.0	2.3
	1156.9		6.4	1.3
16	2200	1 CEM, 1 AEM, 1 BPM	9.2	1.9
17	532.1	1 CEM 1 BPM	3.0	0.6
	429.2		2.4	0.5
	575.3		3.2	0.7
18	1282.7	1 CEM 1 AEM 1 BPM	5.3	1.1
	785.7		3.3	0.7

References	Productivity (mmol N m^{-2} h^{-1})	Membranes used[a]	Productivity (mmol N $\$^{-1}$ membrane h^{-1})[b]	Capital-cost-based productivity (mmol N $\$^{-1}$ h^{-1})[c]
Average	2017.2		10.9	2.3
Flow-electrode capacitive deionization				
19	107.7	1 CEM 1 AEM	0.9	0.2
	81.3		0.7	0.1
	64.9		0.5	0.1
20	39.6	1 CEM 1 AEM	0.3	0.07
	787.8		6.6	1.4
21	38.2	1 CEM, 1 AEM	0.3	0.07
22	66.9	1 CEM, 1 AEM	0.6	0.1
23	190.7	1 CEM 1 AEM	1.6	0.3
	279.0		2.3	0.5
Average	184.0		1.5	0.3
Proton-coupled electron transfer				
24	88.3	2 CEMs	0.7	0.2
	100.7		0.8	0.2
	115.1		1.0	0.2
Average	101.3		0.8	0.2
Prussian blue analogues (electrode)				
25	73.6	1 AEM	1.2	0.3
26	128.1	1 AEM	2.1	0.4
27	128.6	1 AEM	2.1	0.5
	180		3.0	0.6
	205.9		3.4	0.7
28	800	1 AEM	13.3	2.8

References	Productivity (mmol N m^{-2} h^{-1})	Membranes used[a]	Productivity (mmol N $\$^{-1}$ membrane h^{-1})[b]	Capital-cost-based productivity (mmol N $\$^{-1}$ h^{-1})[c]
29	176.3	1 AEM	2.9	0.6
	529.9		8.8	1.9
	660.7		11.0	2.3
	476.7		7.9	1.7
Average	336.0		5.6	1.2
Prussian blue analogues (membrane)				
30	39.7	1 CEM	0.7	0.1
	61.1		1.0	0.2
Average	50.4		0.8	0.2

[a]For multiple cell-pair configurations, the repeating unit was considered.

[b]The productivity (mmol N $\$^{-1}$ membrane h^{-1}) was calculated from the productivity (mmol N m^{-2} h^{-1}) using the midpoint price of IEMs,[53] which was 60 \$ m^{-2} for a cation exchange membrane or an anion exchange membrane, and 120 \$ m^{-2} for a bipolar membrane as well as the number of membranes used in the repeating unit.

[c]The midpoint contribution of ion exchange membrane (IEM) materials (21%) to the capital cost in representative IEM processes (desalination, resource recovery, and energy storage and chemical production) was used to convert the productivity (mmol N $\$^{-1}$ membrane h^{-1}) to capital-cost-based productivity (mmol N $\$^{-1}$ h^{-1}).[54]

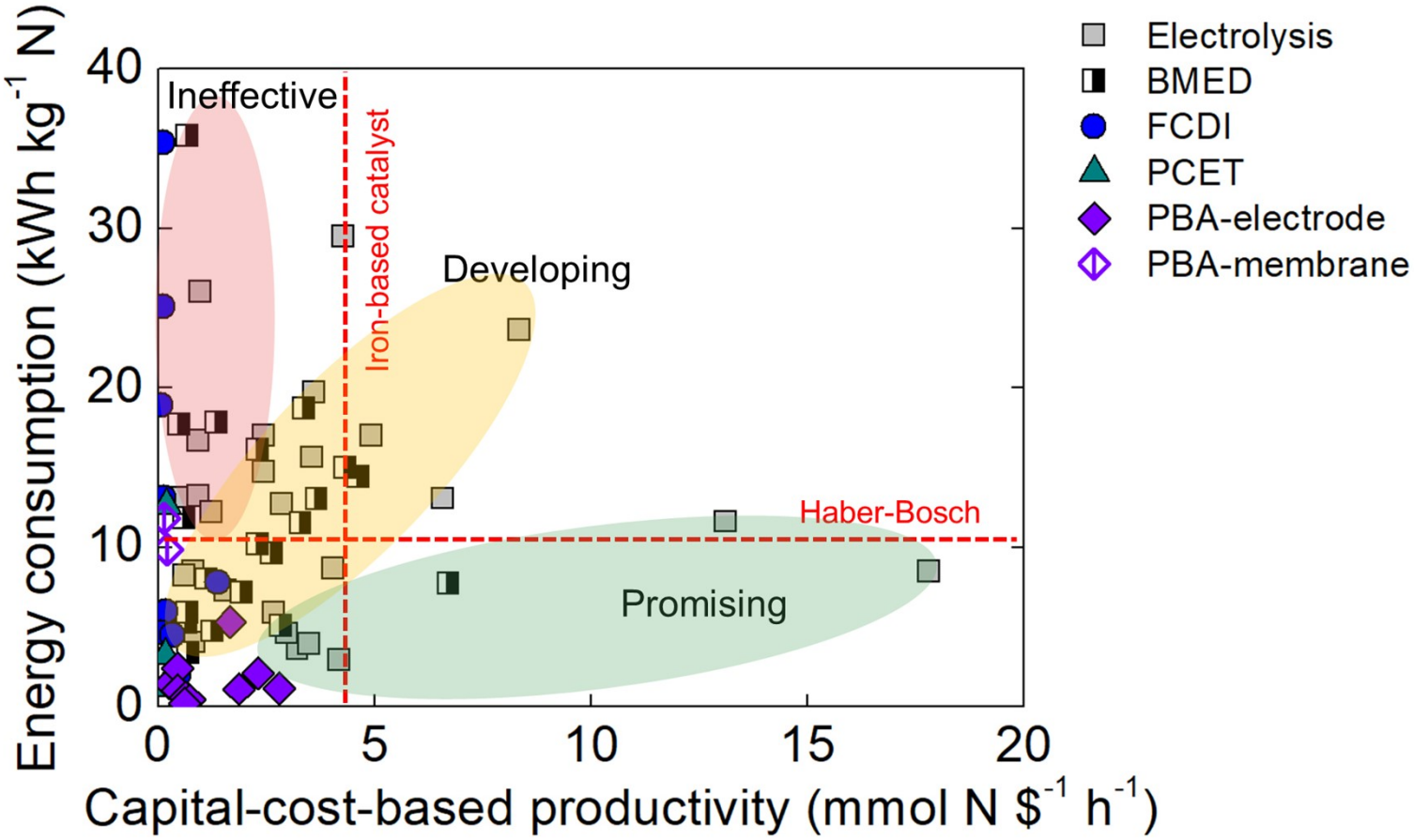

Figure S1. Energy-productivity plot created using the literature data (energy consumption, kWh kg^{-1} N). Two dashed lines indicate the benchmarking energy consumption against the Haber-Bosch process[55] and the average ammonia synthesis rate available from iron-based catalysts (Refs. 31–50). BMED: bipolar membrane electrodialysis; FCDI: flow-electrode capacitive deionization; PCET: proton-coupled electron transfer; PBA: Prussian blue analogue.

References

(1) Desloover, J.; Abate Woldeyohannis, A.; Verstraete, W.; Boon, N.; Rabaey, K. Electrochemical Resource Recovery from Digestate to Prevent Ammonia Toxicity during Anaerobic Digestion. *Environ. Sci. Technol.* **2012**, *46*, 12209–12216. https://doi.org/10.1021/es3028154.

(2) Luther, A. K.; Desloover, J.; Fennell, D. E.; Rabaey, K. Electrochemically Driven Extraction and Recovery of Ammonia from Human Urine. *Water Res.* **2015**, *87*, 367–377. https://doi.org/10.1016/j.watres.2015.09.041.

(3) Christiaens, M. E. R.; Gildemyn, S.; Matassa, S.; Ysebaert, T.; De Vrieze, J.; Rabaey, K. Electrochemical Ammonia Recovery from Source-Separated Urine for Microbial Protein Production. *Environ. Sci. Technol.* **2017**, *51*, 13143–13150. https://doi.org/10.1021/acs.est.7b02819.

(4) Kuntke, P.; Rodríguez Arredondo, M.; Widyakristi, L.; ter Heijne, A.; Sleutels, T. H. J. A.; Hamelers, H. V. M.; Buisman, C. J. N. Hydrogen Gas Recycling for Energy Efficient Ammonia Recovery in Electrochemical Systems. *Environ. Sci. Technol.* **2017**, *51*, 3110–3116. https://doi.org/10.1021/acs.est.6b06097.

(5) Rodríguez Arredondo, M.; Kuntke, P.; ter Heijne, A.; Hamelers, H. V. M.; Buisman, C. J. N. Load Ratio Determines the Ammonia Recovery and Energy Input of an Electrochemical System. *Water Res.* **2017**, *111*, 330–337. https://doi.org/10.1016/j.watres.2016.12.051.

(6) Tarpeh, W. A.; Barazesh, J. M.; Cath, T. Y.; Nelson, K. L. Electrochemical Stripping to Recover Nitrogen from Source-Separated Urine. *Environ. Sci. Technol.* **2018**, *52*, 1453–1460. https://doi.org/10.1021/acs.est.7b05488.

(7) Christiaens, M. E. R.; Udert, K. M.; Arends, J. B. A.; Huysman, S.; Vanhaecke, L.; McAdam, E.; Rabaey, K. Membrane Stripping Enables Effective Electrochemical Ammonia Recovery from Urine While Retaining Microorganisms and Micropollutants. *Water Res.* **2019**, *150*, 349–357.

(8) Aung, S. L.; Choi, J.; Cha, H.; Woo, G.; Song, K. G. Ammonia-Selective Recovery from Anaerobic Digestate Using Electrochemical Ammonia Stripping Combined with Electrodialysis. *Chem. Eng. J.* **2024**, *479*, 147949. https://doi.org/10.1016/j.cej.2023.147949.

(9) Liu, F.; Moustafa, H.; He, Z. Simultaneous Recovery of Nitrogen and Phosphorus from Actual Digester Centrate in an Electrochemical Membrane System. *Resour. Conserv. Recycl.* **2024**, *203*, 107463. https://doi.org/10.1016/j.resconrec.2024.107463.

(10) Kogler, A.; Sharma, N.; Tiburcio, D.; Gong, M.; Miller, D. M.; Williams, K. S.; Chen, X.; Tarpeh, W. A. Long-Term Robustness and Failure Mechanisms of Electrochemical Stripping for Wastewater Ammonia Recovery. *ACS Environ. Au* **2024**, *4*, 89–105. https://doi.org/10.1021/acsenvironau.3c00058.

(11) Choi, S.; Lee, W.; Kim, H.; Lee, G.; Lee, C.; Cheong, D.-Y.; Son, W.-K.; Kim, K. Ammonia Concentration and Recovery in an Up-Scaled Electrochemical Cell through Screening of Cation Exchange Membrane. *Front. Water* **2024**, *6*, 1367315. https://doi.org/10.3389/frwa.2024.1367315.

(12) van Linden, N.; Bandinu, G. L.; Vermaas, D. A.; Spanjers, H.; van Lier, J. B. Bipolar Membrane Electrodialysis for Energetically Competitive Ammonium Removal and Dissolved Ammonia Production. *J. Clean. Prod.* **2020**, *259*, 120788. https://doi.org/10.1016/j.jclepro.2020.120788.

(13) Rodrigues, M.; de Mattos, T. T.; Sleutels, T.; ter Heijne, A.; Hamelers, H. V. M.; Buisman, C. J. N.; Kuntke, P. Minimal Bipolar Membrane Cell Configuration for Scaling Up Ammonium Recovery. *ACS Sustain. Chem. Eng.* **2020**, *8*, 17359–17367. https://doi.org/10.1021/acssuschemeng.0c05043.

(14) Mohammadi, M.; Guo, H.; Yuan, P.; Pavlovic, V.; Barber, J.; Kim, Y. Ammonia Separation from Wastewater Using Bipolar Membrane Electrodialysis. *Electrochem. Sci. Adv.* **2021**, *1*, e2000030. https://doi.org/10.1002/elsa.202000030.

(15) Guo, H.; Yuan, P.; Pavlovic, V.; Barber, J.; Kim, Y. Ammonium Sulfate Production from Wastewater and Low-Grade Sulfuric Acid Using Bipolar- and Cation-Exchange Membranes. *J. Clean. Prod.* **2021**, *285*, 124888. https://doi.org/10.1016/j.jclepro.2020.124888.

(16) Li, Y.; Wang, R.; Shi, S.; Cao, H.; Yip, N. Y.; Lin, S. Bipolar Membrane Electrodialysis for Ammonia Recovery from Synthetic Urine: Experiments, Modeling, and Performance Analysis. *Environ. Sci. Technol.* **2021**, *55*, 14886–14896. https://doi.org/10.1021/acs.est.1c05316.

(17) Ferrari, F.; Pijuan, M.; Molenaar, S.; Duinslaeger, N.; Sleutels, T.; Kuntke, P.; Radjenovic, J. Ammonia Recovery from Anaerobic Digester Centrate Using Onsite Pilot Scale Bipolar Membrane Electrodialysis Coupled to Membrane Stripping. *Water Res.* **2022**, *218*, 118504. https://doi.org/10.1016/j.watres.2022.118504.

(18) Chen, W.; Grimberg, S.; Rogers, S.; Kim, T. Bipolar Membrane Electrodialysis for Nutrient Recovery from Anaerobic Digestion Dewatering Sidestream. *Chem. Eng. J.* **2024**, *488*, 150834. https://doi.org/10.1016/j.cej.2024.150834.

(19) Zhang, C.; Ma, J.; He, D.; Waite, T. D. Capacitive Membrane Stripping for Ammonia Recovery (CapAmm) from Dilute Wastewaters. *Environ. Sci. Technol. Lett.* **2018**, *5*, 43–49. https://doi.org/10.1021/acs.estlett.7b00534.

(20) Zhang, C.; Ma, J.; Song, J.; He, C.; Waite, T. D. Continuous Ammonia Recovery from Wastewaters Using an Integrated Capacitive Flow Electrode Membrane Stripping System. *Environ. Sci. Technol.* **2018**, *52*, 14275–14285. https://doi.org/10.1021/acs.est.8b02743.

(21) Fang, K.; Gong, H.; He, W.; Peng, F.; He, C.; Wang, K. Recovering Ammonia from Municipal Wastewater by Flow-Electrode Capacitive Deionization. *Chem. Eng. J.* **2018**, *348*, 301–309. https://doi.org/10.1016/j.cej.2018.04.128.

(22) Zhang, C.; Ma, J.; Waite, T. D. Ammonia-Rich Solution Production from Wastewaters Using Chemical-Free Flow-Electrode Capacitive Deionization. *ACS Sustain. Chem. Eng.* **2019**, *7*, 6480–6485. https://doi.org/10.1021/acssuschemeng.9b00314.

(23) Chen, T.; Xu, L.; Wei, S.; Tang, X.; Chen, H. Enhanced Ammonia-Rich Solution Production and Electrode Separation Using Magnetic Nickel-Loaded Carbon Black in Flow-Electrode Electrochemical Deionization (FEED). *Desalination* **2022**, *544*, 116152. https://doi.org/10.1016/j.desal.2022.116152.

(24) Chen, W.; Grimberg, S.; Rogers, S.; Kim, T. Ammonia Recovery from Domestic Wastewater Using a Proton-Mediated Redox Couple. *ACS Sustain. Chem. Eng.* **2021**, *9*, 12699–12707. https://doi.org/10.1021/acssuschemeng.1c05144.

(25) Kim, T.; Gorski, C. A.; Logan, B. E. Ammonium Removal from Domestic Wastewater Using Selective Battery Electrodes. *Environ. Sci. Technol. Lett.* **2018**, *5*, 578–583. https://doi.org/10.1021/acs.estlett.8b00334.

(26) Son, M.; Aronson, B. L.; Yang, W.; Gorski, C. A.; Logan, B. E. Recovery of Ammonium and Phosphate Using Battery Deionization in a Background Electrolyte. *Environ. Sci.: Water Res. Technol.* **2020**, *6*, 1688–1696. https://doi.org/10.1039/D0EW00183J.

(27) Son, M.; Kolvek, E.; Kim, T.; Yang, W.; Vrouwenvelder, J. S.; Gorski, C. A.; Logan, B. E. Stepwise Ammonium Enrichment Using Selective Battery Electrodes. *Environ. Sci.: Water Res. Technol.* **2020**, *6*, 1649–1657. https://doi.org/10.1039/D0EW00010H.

(28) Wang, Q.; Wu, Q.; Meng, S.; Liu, H.; Liang, D. Selective Removal of Ammonium Ions with Transition Metal Hexacyanoferrate (MHCF) Electrodes. *Desalination* **2023**, *558*, 116646. https://doi.org/10.1016/j.desal.2023.116646.

(29) Tsai, S.-W.; Cuong, D. V.; Hou, C.-H. Selective Capture of Ammonium Ions from Municipal

Wastewater Treatment Plant Effluent with a Nickel Hexacyanoferrate Electrode. *Water Res.* **2022**, *221*, 118786. https://doi.org/10.1016/j.watres.2022.118786.

(30) Chen, W.; Akinyemi, P.; Kim, T. Selective Separation of Ammonium from Wastewater Using Ion Conducting Channels of a Prussian Blue Analogue. *Environ. Sci. Technol. Lett.* **2024**, *11*, 280–286. https://doi.org/10.1021/acs.estlett.3c00932.

(31) Murakami, K.; Tanaka, Y.; Sakai, R.; Toko, K.; Ito, K.; Ishikawa, A.; Higo, T.; Yabe, T.; Ogo, S.; Ikeda, M.; Tsuneki, H.; Nakai, H.; Sekine, Y. The Important Role of N_2H Formation Energy for Low-Temperature Ammonia Synthesis in an Electric Field. *Catal. Today* **2020**, *351*, 119–124. https://doi.org/10.1016/j.cattod.2018.10.055.

(32) Gao, W.; Guo, J.; Wang, P.; Wang, Q.; Chang, F.; Pei, Q.; Zhang, W.; Liu, L.; Chen, P. Production of Ammonia via a Chemical Looping Process Based on Metal Imides as Nitrogen Carriers. *Nat. Energy* **2018**, *3*, 1067–1075. https://doi.org/10.1038/s41560-018-0268-z.

(33) Homs, N.; De La Piscina, P. R.; Fierro, J. L. G.; Sueiras, J. E. Catalytic Activity for Ammonia Synthesis of Iron Supported Catalysts Prepared from an Acid-Modified λ-Al_2O_3 Method. *Z. Anorg. Allg. Chem.* **1984**, *518*, 227–233. https://doi.org/10.1002/zaac.19845181123.

(34) Smith, P. J.; Taylor, D. W.; Dowden, D. A.; Kemball, C.; Taylor, D. Ammonia Synthesis and Related Reactions over Iron-Cobalt and Iron-Nickel Alloy Catalysts: Part II. Catalysts Reduced above 853 K. *Appl. Catal.* **1982**, *3*, 303–314. https://doi.org/10.1016/0166-9834(82)80265-0.

(35) Kitano, M.; Kujirai, J.; Ogasawara, K.; Matsuishi, S.; Tada, T.; Abe, H.; Niwa, Y.; Hosono, H. Low-Temperature Synthesis of Perovskite Oxynitride-Hydrides as Ammonia Synthesis Catalysts. *J. Am. Chem. Soc.* **2019**, *141*, 20344–20353. https://doi.org/10.1021/jacs.9b10726.

(36) Baiker, A.; Baris, H.; Schlögl, R. Ammonia Synthesis over a Supported Iron Catalyst Prepared from an Amorphous Iron-Zirconium Precursor: III. Mechanism of Nitrogen Adsorption and Ammonia Synthesis Kinetics. *J. Catal.* **1987**, *108*, 467–479. https://doi.org/10.1016/0021-9517(87)90194-1.

(37) Wang, P.; Xie, H.; Guo, J.; Zhao, Z.; Kong, X.; Gao, W.; Chang, F.; He, T.; Wu, G.; Chen, M.; Jiang, L.; Chen, P. The Formation of Surface Lithium–Iron Ternary Hydride and Its Function on Catalytic Ammonia Synthesis at Low Temperatures. *Angew. Chem., Int. Ed.* **2017**, *56*, 8716–8720. https://doi.org/10.1002/anie.201703695.

(38) Wang, P.; Chang, F.; Gao, W.; Guo, J.; Wu, G.; He, T.; Chen, P. Breaking Scaling Relations to Achieve Low-Temperature Ammonia Synthesis through LiH-Mediated Nitrogen Transfer and Hydrogenation. *Nat. Chem.* **2017**, *9*, 64–70. https://doi.org/10.1038/nchem.2595.

(39) Hagen, S.; Barfod, R.; Fehrmann, R.; Jacobsen, C. J.; Teunissen, H. T.; Chorkendorff, I. Ammonia Synthesis with Barium-Promoted Iron–Cobalt Alloys Supported on Carbon. *J. Catal.* **2003**, *214*, 327. https://doi.org/10.1016/s0021-9517(02)00182-3.

(40) Humphreys, J.; Lan, R.; Chen, S.; Tao, S. Improved Stability and Activity of Fe-Based Catalysts through Strong Metal Support Interactions Due to Extrinsic Oxygen Vacancies in $Ce_{0.8}Sm_{0.2}O_{2-\delta}$ for the Efficient Synthesis of Ammonia. *J. Mater. Chem. A* **2020**, *8*, 16676–16689. https://doi.org/10.1039/D0TA05238H.

(41) Morlanés, N.; Almaksoud, W.; Rai, R. K.; Ould-Chikh, S.; Ali, M. M.; Vidjayacoumar, B.; Al-Sabban, B. E.; Albahily, K.; Basset, J.-M. Development of Catalysts for Ammonia Synthesis Based on Metal Phthalocyanine Materials. *Catal. Sci. Technol.* **2020**, *10*, 844–852. https://doi.org/10.1039/C9CY02326G.

(42) Yan, P.; Guo, W.; Liang, Z.; Meng, W.; Yin, Z.; Li, S.; Li, M.; Zhang, M.; Yan, J.; Xiao, D.; Zou, R.; Ma, D. Highly Efficient K-Fe/C Catalysts Derived from Metal-Organic Frameworks towards Ammonia

Synthesis. *Nano Res.* **2019**, *12*, 2341–2347. https://doi.org/10.1007/s12274-019-2349-0.

(43) Jafari, A.; Ebadi, A.; Sahebdelfar, S. Effect of Iron Oxide Precursor on the Properties and Ammonia Synthesis Activity of Fused Iron Catalysts. *React. Kinet. Mech. Catal.* **2019**, *126*, 307–325. https://doi.org/10.1007/s11144-018-1498-6.

(44) Tang, Y.; Kobayashi, Y.; Masuda, N.; Uchida, Y.; Okamoto, H.; Kageyama, T.; Hosokawa, S.; Loyer, F.; Mitsuhara, K.; Yamanaka, K.; Tamenori, Y.; Tassel, C.; Yamamoto, T.; Tanaka, T.; Kageyama, H. Metal-Dependent Support Effects of Oxyhydride-Supported Ru, Fe, Co Catalysts for Ammonia Synthesis. *Adv. Energy Mater.* **2018**, *8*, 1801772. https://doi.org/10.1002/aenm.201801772.

(45) Fan, H.; Huang, X.; Kähler, K.; Folke, J.; Girgsdies, F.; Teschner, D.; Ding, Y.; Hermann, K.; Schlögl, R.; Frei, E. In-Situ Formation of Fe Nanoparticles from FeOOH Nanosheets on γ-Al_2O_3 as Efficient Catalysts for Ammonia Synthesis. *ACS Sustain. Chem. Eng.* **2017**, *5*, 10900–10909. https://doi.org/10.1021/acssuschemeng.7b02812.

(46) Liu, H.; Liu, C.; Li, X.; Cen, Y. Effect of an Iron Oxide Precursor on the H_2 Desorption Performance for an Ammonia Synthesis Catalyst. *Ind. Eng. Chem. Res.* **2003**, *42*, 1347–1349. https://doi.org/10.1021/ie0202524.

(47) Kowalczyk, Z.; Jodzis, S. Activity and Thermoresistance of Fused Iron Catalysts for Ammonia Synthesis. *Appl. Catal.* **1990**, *58*, 29–34. https://doi.org/10.1016/S0166-9834(00)82276-9.

(48) Liu, H.-Z.; Li, X.-N.; Hu, Z.-N. Development of Novel Low Temperature and Low Pressure Ammonia Synthesis Catalyst. *Appl. Catal. A Gen.* **1996**, *142*, 209–222. https://doi.org/10.1016/0926-860X(96)00047-6.

(49) Spencer, N. Iron Single Crystals as Ammonia Synthesis Catalysts: Effect of Surface Structure on Catalyst Activity. *J. Catal.* **1982**, *74*, 129–135. https://doi.org/10.1016/0021-9517(82)90016-1.

(50) Brown, D. E.; Edmonds, T.; Joyner, R. W.; McCarroll, J. J.; Tennison, S. R. The Genesis and Development of the Commercial BP Doubly Promoted Catalyst for Ammonia Synthesis. *Catal. Lett.* **2014**, *144*, 545–552. https://doi.org/10.1007/s10562-014-1226-4.

(51) Yoshida, M.; Ogawa, T.; Ishihara, K. N. Economic Limitation of Recent Heterogeneous Catalysts for Ammonia Synthesis. *Clean. Chem. Eng.* **2024**, *10*, 100119. https://doi.org/10.1016/j.clce.2024.100119.

(52) Bañares-Alcántara, R.; Iii, G. D.; Fiaschetti, M.; Grünewald, P.; Lopez, J. M.; Tsang, E.; Yang, A.; Ye, L.; Zhao, S. Analysis of Islanded Ammonia-Based Energy Storage Systems. *University of Oxford* **2015**.

(53) Hand, S.; Guest, J. S.; Cusick, R. D. Technoeconomic Analysis of Brackish Water Capacitive Deionization: Navigating Tradeoffs between Performance, Lifetime, and Material Costs. *Environ. Sci. Technol.* **2019**, *53*, 13353–13363. https://doi.org/10.1021/acs.est.9b04347.

(54) Reimonn, G.; Kamcev, J. Techno-Economic Perspective on the Limitations and Prospects of Ion-Exchange Membrane Technologies. *Curr. Opin. Chem. Eng.* **2025**, *47*, 101077. https://doi.org/10.1016/j.coche.2024.101077.

(55) Maurer, M.; Schwegler, P.; Larsen, T. A. Nutrients in Urine: Energetic Aspects of Removal and Recovery. *Water Sci. Technol.* **2003**, *48*, 37–46. https://doi.org/10.2166/wst.2003.0011.